Harmonic susceptibilities of a sintered oxide superconductor

K. Yamamoto
Ube Laboratory, Ube Industries Ltd., Ube 755, Japan

H. Mazaki and H. Yasuoka
Department of Mathematics and Physics, The National Defense Academy, Yokosuka 239, Japan

S. Katsuyama
Department of Material Science and Engineering, Faculty of Engineering, Osaka University, Suita 565, Japan

K. Kosuge
Department of Chemistry, Faculty of Science, Kyoto University, Kyoto 606, Japan
(Received 3 September 1991)

The superconducting transition of a sintered $YBa_2Cu_3O_y$ pellet with Fe impurities was measured in terms of harmonic susceptibilities $\chi_n=\chi_n'-i\chi_n''$ ($n=1$, 2, 3, 5, and 7). The results were analyzed in the framework of the critical-state model and the weak-link model. Generation of the higher-harmonic susceptibilities seems to arise from the supercurrent according to the Kim-Anderson critical-state model, while the Ishida-Mazaki weak-link model, based on the assumption that the intergrain network behaves like a single loop as a whole due to its coherent nature, fails to describe the data. However, phenomenological considerations suggest that the extended weak-link model, in which a number of coaxial weak-link loops are assumed in the specimen, would be more practical for analyses of the magnetic response of oxide ceramic superconductors prepared by sintering.

I. INTRODUCTION

The measurement of the complex susceptibility $\chi=\chi'-i\chi''$ in a weak ac magnetic field is one of the useful probes for the study of the magnetic response of superconductors.[1-4] For conventional bulk superconductors, χ' exhibits a sharp decrease just below the critical temperature T_c and χ'' forms a peak in the temperature region of the superconducting transition. For sintered high-T_c superconductors, it is well known that χ involves two components: the intragrain bulk component and the intergrain coupling component. These two components typically can be accessed by changing the amplitude of the ac measuring field H_{ac}. The intragrain bulk component is insensitive to the change in H_{ac}, while the coupling component varies even for a slight change in field amplitude of only 10^{-4} mT.[5] These observations, together with the resistive transition, are indispensable for characterizing the superconducting properties.

The time-dependent magnetization $M(\omega t)$ of a specimen for a magnetic field,

$$H(\omega t)=H_{dc}+H_{ac}\mathrm{Re}[\exp(i\omega t)] ,$$

generally can be expressed in the form of a Fourier expansion:

$$M(\omega t)=\chi_0 H_{dc}+H_{ac}\sum_{n=1}^{\infty}\mathrm{Re}[\chi_n\exp(in\omega t)] , \quad (1)$$

where Re[ ] denotes the real part of a complex variable and $\omega=2\pi f_1$, where f_1 is the fundamental frequency. The first term $\chi_0 H_{dc}$ is an offset by a dc magnetic field H_{dc}, and the second is the ac component which varies in time with the ac magnetic field $H_{ac}\cos(\omega t)$. Here we define the harmonic ac susceptibility $\chi_n=\chi_n'-i\chi_n''$, ($n=1,2,3,\ldots$) as the Fourier coefficients of the magnetization, where χ_1 is the fundamental susceptibility and the others are the higher-harmonic susceptibilities.

To elucidate the generation of higher-harmonic components, several models have been proposed. These are roughly divided into two categories. One is based on the critical-state model, introduced by Bean on the assumption that the critical-current density is independent of field.[6] In his model the existence of odd-n harmonic susceptibilities can be derived. Bean's approach was extended by Kim, Hempstead, and Strnad[7] and Anderson,[8] who assumed that every region of the sample carries a critical-current density determined by the local magnetic field. In this model one can derive only odd-n harmonics when a pure ac field is applied to a superconductor. But if a dc field is superimposed on the ac field, even-n harmonics are generated.

The second category for which higher-harmonic susceptibilities are predicted is the so-called weak-link model, which was proposed by Ishida and Mazaki for a multiconnected microbridge network of low-temperature superconductors.[9] The expressions derived from this model are equivalent to those of Rollins and Silcox.[10] The weak-link model proved the existence of odd-n harmonic susceptibilities and qualitatively explained the profiles of χ_n versus temperature observed for weakly coupled networks.

Recently, Ishida and Goldfarb carried out detailed measurements and analyses of χ_n ($n=1,2,\ldots,10$) for a sintered $YBa_2Cu_3O_y$ (YBCO) superconductor where they superimposed a dc field H_{dc} on an ac field.[11] They found that the χ_1' transition curve initially shifts to higher temperatures with increasing H_{dc} and that both the even- and odd-n harmonics emerge for nonzero H_{dc}. They analyzed the results with a simplified Kim model for the critical-current density[12] and found that the temperature- and field-dependent features of χ_n were in good agreement with the model calculations.

The substitution for Cu in YBCO by other metals is an attractive method to obtain fundamental information on this class of materials. It is expected that the crystal structure and superconductivity of impurity-doped YBCO would be strongly affected by the species and distribution of dopant atoms. With this viewpoint, we have recently studied the superconducting properties of Fe-doped YBCO, $YBa_2(Cu_{1-x}Fe_x)_3O_y$, in terms of the fundamental susceptibility χ_1.[13] As one of the conclusions of that study, we found that the Fe-doped sample treated by a conventional oxidization process had almost the same characteristics as pure YBCO without Fe impurities, except for the transition temperature.

To get more detailed information on the magnetic response of sintered oxide superconductors, it is worthwhile to measure the higher-harmonic susceptibilities χ_n and to analyze the observed results by model calculations. In the present study, we chose one of these Fe-doped samples ($x=0.06$) and measured χ_n ($n=1$, 2, 3, 5, and 7). We present the details of the measurement together with the observed χ_n as a function of temperature. Analyses of the data were carried out in the framework of the Kim-Anderson[7,8] and Ishida-Mazaki[9] models.

II. EXPERIMENTAL DETAILS

A. Sample preparation

Since the details of the sample preparation and its characterization have been reported previously,[13,14] we give here only a brief outline. The sample was fabricated by a solid-state reaction of 99.99%-pure Y_2O_3, $BaCO_3$, CuO, and α-Fe_2O_3. The mixture was pelletized, heated at 900 °C in air for 24 h, ground, and reheated. This process was repeated several times, and finally the product was sintered at 930 °C in air for 24 h. The material thus prepared was treated by a conventional oxidization process (slow cooling from 850 °C in flowing O_2 gas). Phase identification of the sample was made by powder x-ray diffraction, and the specimen was found to be single phase, where the phase transition from orthorhombic to tetragonal symmetry occurs at around $x=0.02-0.04$ [see Fig. 1(a) of Ref. 13]. The fundamental ac susceptibilities of these Fe-doped samples show essentially the same profiles as that of a YBCO sample without Fe, although the superconducting transition temperature becomes lower as x increases (see Fig. 2 of Ref. 13).

The specimen used here for the measurement of χ_n ($x=0.06$) is a superconductor with tetragonal symmetry. It has the typical magnetic response seen for conventional oxide superconductors prepared by sintering. We emphasize that, in the present study, the use of a *sintered* sample is essential, and the effect of Fe doping is not explicitly taken into consideration.

B. Measurements of χ_n

A schematic diagram of the measuring system for higher-harmonic susceptibilities is shown in Fig. 1. The system consists of a Hartshorn bridge, a two-phase lock-in amplifier, and two function generators. In the measurement of χ_n as a function of temperature, the sample temperature was varied quite slowly, typically less than 0.3 K/min to avoid a temperature gradient inside the sample. The null adjustment of the bridge for the fundamental frequency and the phase setting between the applied magnetic field and reference signal were made at a temperature slightly above T_c. Phase setting with the sample *in situ* is very important for accurate separation of the real and imaginary components of χ_n.

The ac magnetic field $H_{ac}\cos(\omega t)$ was applied to the sample using function generator $F1$; the second generator $F2$ was used to generate the nth-harmonic sinusoidal wave synchronized with $F1$. By means of Lissajous figures on an oscilloscope, we confirmed that no phase shift occurred during each run of the measurement. The amplitude of the ac magnetic field $\mu_0 H_{ac}$ in units of teslas was in the range 0.01–0.1 mT, where $\mu_0=4\pi\times10^{-7}$ H/m, and f_1 was typically 132 Hz. In this experiment magnetic shielding was not used, and so the applied ac field was superimposed on the Earth's field, even when the applied dc field was zero.

Since the bridge was balanced at a sample temperature above T_c, the off-balance signal $v(\omega t)$, induced in the secondary circuit by decreasing temperature, is directly proportional to the time derivative of the sample magnetization $M(\omega t)$. Using Eq. (1), we get

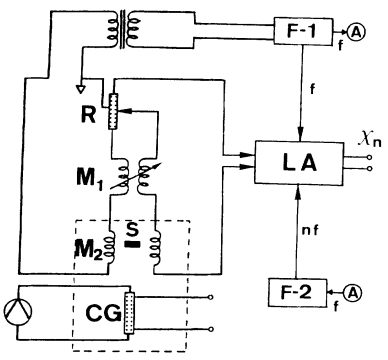

FIG. 1. Schematic diagram of the measuring system: M_1, variable standard mutual inductance; M_2, cryostat coil; R, phase-shift potentiometer; S, sample; CG, carbon-glass thermometer; $F1$,$F2$, function generators; LA, lock-in amplifier.

$$v(\omega t)=-\gamma\frac{dM(\omega t)}{dt}$$
$$=-\gamma H_{\rm ac}\sum_{n=1}^{\infty}\mathrm{Re}[in\omega\chi_n\exp(in\omega t)]$$
$$=-\gamma H_{\rm ac}\sum_{n=1}^{\infty}n\omega[-\chi_n'\sin(n\omega t)+\chi_n''\cos(n\omega t)]\ , \tag{2}$$

where γ is a constant which depends on the number of turns in the coils and on the volume and shape of the sample, as well as on its position in the coil.

Meanwhile, $v(\omega t)$ can be generally expressed in the form of a Fourier expansion

$$v(\omega t)=\sum_{n=1}^{\infty}\mathrm{Re}[a_n\exp(in\omega t)]\ , \tag{3}$$

where $a_n=a_n'-ia_n''$ $(n=1,2,3,\ldots)$ are the Fourier coefficients which are determined experimentally. From Eqs. (2) and (3), we get the real and imaginary components of the nth-harmonic susceptibilities as $\chi_n'=a_n''/\gamma n\omega H_{\rm ac}$ and $\chi_n''=-a_n'/\gamma n\omega H_{\rm ac}$. In the present case, the Fourier coefficients a_n' and a_n'' were determined with the two-phase lock-in amplifier with which the nth-harmonic terms of $v(\omega t)$ were obtained. The reference signal $v_n\propto\cos(n\omega t)$ was input from $F2$ $(n=3,$ 5, and 7). The fundamental- and second-harmonic terms were measured using the reference signal from $F1$.

Ideally, to obtain an absolute value of χ_n, γ should be calculated by calibrating the susceptometer with a standard sample which has the same volume and shape as the specimen in question. In our case we normalized χ_n to the saturated value of $|\chi_1'|$ in a weak magnetic field ($\mu_0H_{\rm ac}=0.01$ mT, $T=4.2$ K), and γ was determined from $\chi_1'=-1$.

III. MODEL CALCULATIONS

Since the observed curves of χ_n were analyzed in the framework of the Kim-Anderson and Ishida-Mazaki models, we first give brief outlines of these models and then describe the algebraic treatments.

A. Kim-Anderson model

The basic premise of the critical-state model is that, when a magnetic field is applied to a type-II superconductor, a macroscopic supercurrent circulates in the specimen with a critical-current density $J_c(B_i)$, where B_i is the local flux density inside the specimen. Bean derived the full hysteresis loop by assuming that J_c is a constant independent of B_i and predicted a generation of odd-n harmonic susceptibilities.[6]

In principle, $J_c(B_i)$ can have various forms. In the Kim-Anderson model,[7,8] the critical-current density as a function of B_i is assumed to be

$$J_c(B_i)=\frac{k}{B_0+|B_i|}\ , \tag{4}$$

where k and B_0 are constants. As pointed out by Chen and Goldfarb,[15] the relation given by Eq. (4) is a very generalized form of the critical-state model, because it is equivalent to the linear model[16] when $B_0\gg B_i$ and to the Bean model[6] when k and B_0 become infinite in such a way that k/B_0 is a constant. Besides, when $B_0=0$, it leads to the power-law model[17,18] where the power of B_i is -1, the so-called simplified Kim model.[12]

Using Eq. (4), Chen and Goldfarb derived the M-H hysteresis loop for the case with no dc-offset magnetic field.[15] In the present study, we extend their derivation to the case where an ac magnetic field is superimposed on a dc magnetic field and calculate the fundamental and higher-harmonic susceptibilities as a function of temperature T. We emphasize three remarkable points from applying this model. First, if a dc-offset field exists, the generation of even-n harmonic susceptibilities is predicted for the case where B_0 does not diverge to infinity. Second, when the maximum value of applied field, $H_{\rm max}=|H_{\rm ac}|+|H_{\rm dc}|$, i.e., the maximum value of $|B_i|/\mu_0$, is comparable with B_0/μ_0, the behavior of the χ_n-versus-T curves is expected to vary drastically with $H_{\rm max}$, since the distribution of J_c in the specimen becomes sensitive to the change in $H_{\rm max}$. Third, in the extreme case of $B_0=0$ with a fixed $H_{\rm dc}$ (the simplified Kim model) or $B_0\to\infty$ (the Bean model), the relation between χ_n' and χ_n'' is uniquely determined, and consequently no $H_{\rm max}$ dependence appears.

B. Ishida-Mazaki model

A phenomenological model that explains the behavior of χ_n of a granular superconductor connected by intergrain weak-link junctions has been proposed by Ishida and Mazaki.[9] They considered a superconducting loop which closes through the weak-link junctions. When the external magnetic field exceeds a critical value, a magnetic-flux quantum can penetrate into the loop. They assumed that the intergrain multiconnected network behaves like a single loop as a whole because of the coherent nature of the specimen. By this model the main features of the magnetic response of a multiconnected network can be reproduced and odd-n harmonic susceptibilities are predicted.

C. Calculations of χ_n' and χ_n''

When the sample magnetization $M(\omega t)$ is expressed by Eq. (1), the real and imaginary components of χ_n can be calculated by

$$\chi_n'=\frac{1}{\pi H_{\rm ac}}\int_0^{2\pi}M(\omega t)\cos(n\omega t)d(\omega t)\ , \tag{5}$$

$$\chi_n''=\frac{1}{\pi H_{\rm ac}}\int_0^{2\pi}M(\omega t)\sin(n\omega t)d(\omega t)\ . \tag{6}$$

For each model described above, $M(\omega t)$ was derived for a period of the applied external field $H(\omega t)$. Equations for M as a function of H for the Kim-Anderson model are planned to appear elsewhere.[19] In the case of the weak-link model, the supercurrent J flows across the weak link

to shield the specimen against the applied field H. As H increases, J increases until it reaches the critical-current density J_c of the weak link. When J exceeds J_c, a flux quantum penetrates into the loop. Using the critical field H_m determined by J_c, the average magnetization $M(H)$ can be written as follows.

When H decreases from H_{ac} to $-H_{ac}$,

$$M(H)=-H+H_{ac}-H_m \quad \text{for } H\geq H_{ac}-2H_m \ , \tag{7}$$

$$M(H)=H_m \quad \text{for } H_{ac}-2H_m\geq H\geq -H_{ac} \ . \tag{8}$$

When H increases from $-H_{ac}$ to H_{ac},

$$M(H)=-H-H_{ac}+H_m \quad \text{for } H\leq -H_{ac}+2H_m, \tag{9}$$

$$M(H)=-H_m \quad \text{for } -H_{ac}+2H_m\leq H\leq H_{ac}. \tag{10}$$

Using these equations given for each model, we evaluated M. To carry out the evaluation, one period of the alternating magnetic field ($0\leq\omega t\leq 2\pi$) was divided into 360 regular intervals, and $M(\omega t)$ was numerically obtained at each point. Substituting the calculated results of $M(\omega t)$ into Eqs. (5) and (6), we evaluated χ_n' and χ_n''.

The temperature dependence of χ_n is introduced through various T-dependent parameters. The parameter k in the Kim-Anderson model is temperature dependent, but no clear expression has been proposed. Therefore, in the present calculation, we tentatively assumed $k(T/T_c)=k(0)(1-T/T_c)^{3/2}$, where $k(0)$ was chosen to give a similar transition width as the experimental curves. This assumption is based on the fact that when $|B_i|=0$, k is proportional to the critical-current density, and for a tunnel junction, $J_c\propto(1-T/T_c)^{3/2}$ at a temperature near T_c.

In the Ishida-Mazaki model, the critical field H_m, at which the flux begins to penetrate into the weak-link loop, is the temperature-dependent parameter. Taking into consideration that H_m is proportional to the critical-current density, we assume

$$H_m(T/T_c)=H_m(0)(1-T/T_c)^{3/2} \ .$$

$H_m(0)$ was again chosen to fit the transition width to the experimental curves.

It is, of course, possible to assume any other temperature dependence. However, since we focus here our attention to the relative values of χ_n at each temperature, the exact functional relation of these parameters with T is not important.

IV. RESULTS AND DISCUSSION

In Fig. 2 we show χ_1' and χ_1'' versus T observed for two different values of $\mu_0 H_{ac}$, 0.01 and 0.1 mT, where $f_1=132$ Hz and no dc field was applied, $H_{dc}=0$ (not including the Earth's field). The curves of χ_1' versus T show a two-step growth as T decreases. As indicated in the figure, the onset temperature of χ_1' is labeled T_{c1}, and T_{c2} is the temperature at which χ_1' begins a rapid growth (corresponding to the onset temperature of χ_1''). In the temperature region between T_{c1} and T_{c2}, χ_1' is almost independent on the field amplitude H_{ac}. However, below

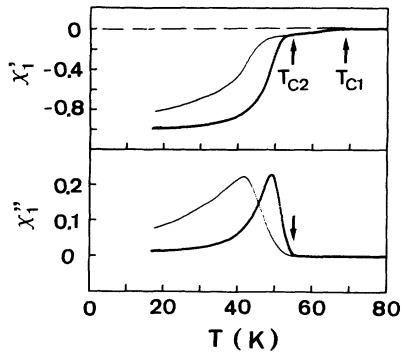

FIG. 2. Real and imaginary components of χ_1 for two different values of $\mu_0 H_{ac}$, 0.01 mT (large dots) and 0.1 mT (small dots), where $f_1=132$ Hz and $H_{dc}=0$.

T_{c2}, χ_1' depends sensitively on H_{ac}, and the temperature where χ_1' saturates becomes lower for a larger value of H_{ac}. χ_1'' forms a single peak in the temperature region below T_{c2}, and the peak width is broadened as H_{ac} increases.

This type of χ_1 profile is common for sintered oxide superconductors[5] and has been qualitatively explained by the weak-link model.[9] According to this model, the specimen consists of small grains coupled by weak links through the grain boundaries. When the specimen is cooled from the normal state, the superconducting grains first become evident at T_{c1}, and the shielding of these grains is detected as a negative χ_1'. This signal, due to the bulk component, is actually insensitive to the small applied field used in the present measurement. In this temperature region, there may be eddy-current losses which contribute to χ_1''. However, it cannot be seen on the scale given in the figure.

With further cooling intergrain coupling occurs at T_{c2}, which is characterized by the quality of grain boundaries, as well as by the volume fraction of grains in the specimen. Below T_{c2}, χ_1' grows rapidly, since the shielding supercurrent begins to circulate in the specimen, and consequently the volume fraction from which the flux is shielded rapidly increases. At extremely low temperatures, the whole volume of the specimen is expected to be shielded by the supercurrent, and thus the χ_1'-versus-T curve saturates. The peak formation of χ_1'' originates from hysteresis loss, for which a phenomenological explanation was made by the weak-link model.[9]

In Figs. 3(a), 4(a), and 5(a), we show χ_n ($n=3$, 5, and 7) versus reduced temperature t_r observed for $\mu_0 H_{ac}=0.01$ mT, $H_{dc}=0$, and $f_1=132$ Hz, where t_r is defined as T/T_{c2}. All of these three χ_n have rather complicated, but nonzero values in the temperature region below T_{c2}. These finite values, together with that of χ_1'' below T_{c2}, indicate that the origin of the higher-harmonic susceptibilities is certainly correlated to the nonlinear response of the sample magnetization against the applied ac field.

Employing the Kim-Anderson model with B_0,

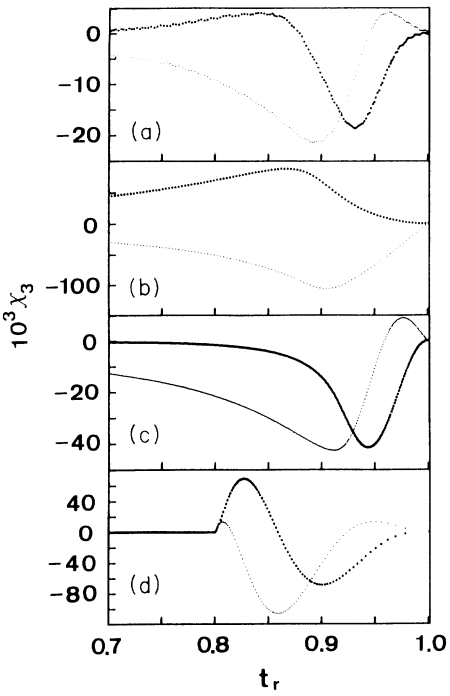

FIG. 3. χ_3 vs reduced temperature t_r: (a) measured for $\mu_0 H_{ac}=0.01$ mT and $f_1=132$ Hz, (b) calculated with use of Kim-Anderson model for $B_0=0$, (c) calculated with the same model for $B_0=1$ mT, and (d) calculated with use of the Ishida-Mazaki model. Large dots represent the real part, and small dots are the imaginary part.

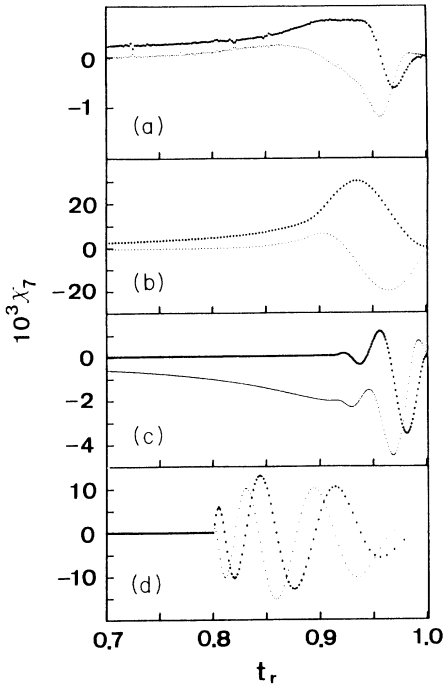

FIG. 5. χ_7 vs reduced temperature t_r: (a) measured for $\mu_0 H_{ac}=0.01$ mT and $f_1=132$ Hz; (b) calculated with use of the Kim-Anderson model for $B_0=0$, (c) calculated with the same model for $B_0=1$ mT, and (d) calculated with use of the Ishida-Mazaki model. Large dots represent the real part, and small dots are the imaginary part.

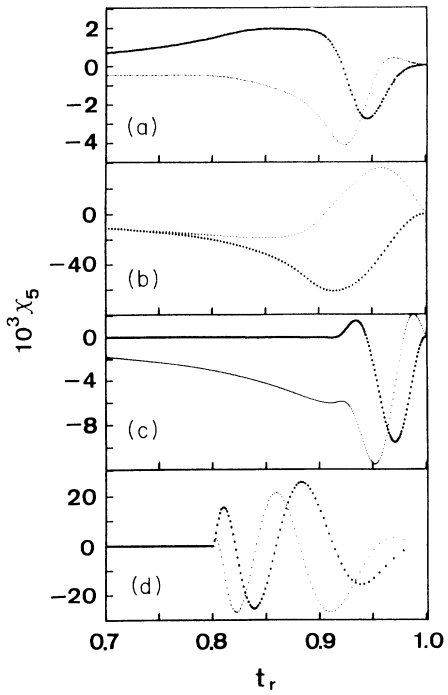

FIG. 4. χ_5 vs reduced temperature t_r: (a) measured for $\mu_0 H_{ac}=0.01$ mT and $f_1=132$ Hz, (b) calculated with use of the Kim-Anderson model for $B_0=0$, (c) calculated with the same model for $B_0=1$ mT, and (d) calculated with use of the Ishida-Mazaki model. Large dots represent the real part, and small dots are the imaginary part.

Müller[20] calculated the fundamental ac susceptibility for a sintered bulk YBCO superconductor, where the intergranular and intragranular pinning forces are assumed to be independent of the local flux density. As described in the preceding section, we attempt to reproduce the observed higher-harmonic susceptibilities in the framework of the Kim-Anderson and Ishida-Mazaki models. Comparison of the observed χ_n-t_r curves with the calculated results show that the Kim-Anderson model with $B_0=1$ mT can reproduce fairly well the experimental profiles. However, the absolute values of measured χ_n [Figs. 3(a), 4(a), and 5(a)] are quantitatively smaller than the calculated χ_n [Figs. 3(c), 4(c), and 5(c)]. The main reason for this discrepancy may come from the different normalization factor $|\chi_1'|$. $|\chi_1'|$ for the measured χ_n ultimately involves both the intragrain bulk and intergrain coupling components, while $|\chi_1'|$ used for calculating χ_n is based solely the intergrain coupling component.

From the above results in Figs. 3–5, we suggest that the Kim-Anderson model with a *finite* value of B_0 is able to simulate the higher-harmonic susceptibilities of sintered oxide superconductors. To find the lower limit of B_0, it is preferable to measure χ_n for a larger value of field amplitude H_{ac}. The reason is that, as mentioned in the preceding section, the χ_n-t_r behavior should change drastically when the maximum applied field $H_{max}=|H_{ac}|+|H_{dc}|$ (i.e., the maximum value of $|B_i|/\mu_0$) becomes comparable with B_0/μ_0. For this purpose we measured χ_n ($n=3$, 5, and 7) versus t_r, for $\mu_0 H_{ac}=0.1$

mT, $H_{dc}=0$, and $f_1=132$ Hz. The results are shown in Figs. 6(a), 7(a), and 8(a). Compared with the results for $\mu_0 H_{ac}=0.01$ mT, we find that the profiles of χ_n-t_r curves do not exhibit any notable change, although they seem to be broadened as a whole. The similarity of these observations for $\mu_0 H_{ac}=0.01$ and 0.1 mT suggests that B_0 must be much larger than 0.1 mT.

The above speculation can be indirectly supported by substituting different values of B_0 into Eq. (4). Using three different values of B_0 (0.1, 1, and 10 mT), we deduced the χ_n-t_r curves. As presented in the lower three plots in Figs. 6–8, we again find that a finite value of B_0 reproduces well the observed results.

The upper limit of B_0 may be roughly estimated from the second-harmonic susceptibility χ_2. In a zero dc magnetic field, even-n harmonic susceptibilities cannot be derived by any model so far reported. As shown in Fig. 9, however, we found apparent nonzero values of χ_2 below T_{c2}, although the absolute values of χ_2 are much smaller than those of odd-n harmonic susceptibilities. We believe the observed χ_2 term is certainly caused by the Earth's field. According to the Kim-Anderson model,[7,8] even-n harmonic susceptibilities emerge when a finite dc field is superimposed on an ac field. On the contrary, the Ishida-Mazaki model[9] cannot generate even-n harmonic terms even under a superimposed dc field.

In Fig. 10 we show χ_2-t_r curves calculated by the Kim-Anderson model with $B_0=0.1$, 1, and 10 mT, where we assume $\mu_0 H_{ac}=0.01$ mT and $\mu_0 H_{dc}=-0.01$ mT. As

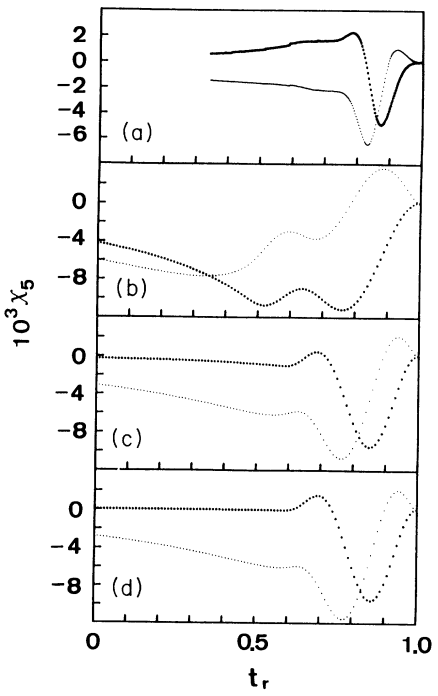

FIG. 7. χ_5 vs reduced temperature t_r: (a) measured for $\mu_0 H_{ac}=0.1$ mT and $f_1=132$ Hz and (b),(c),(d) calculated with use of the Kim-Anderson model for $B_0=0.1$, 1, and 10 mT, respectively. Large dots represent the real part, and small dots are the imaginary part.

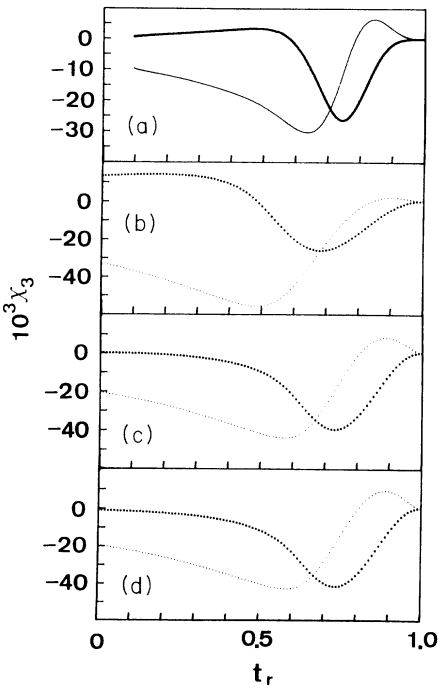

FIG. 6. χ_3 vs reduced temperature t_r: (a) measured for $\mu_0 H_{ac}$0.1 mT and $f_1=132$ Hz and (b),(c),(d) calculated with use of the Kim-Anderson model for $B_0=0.1$, 1, and 10 mT, respectively. Large dots represent the real part, and small dots are the imaginary part.

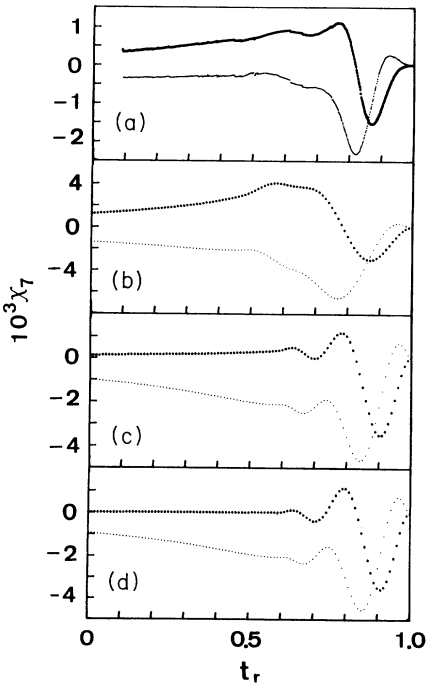

FIG. 8. χ_7 vs reduced temperature t_r: (a) measured for $\mu_0 H_{ac}=0.1$ mT and $f_1=132$ Hz and (b),(c),(d) calculated with use of the Kim-Anderson model for $B_0=0.1$, 1, and 10 mT, respectively. Large dots represent the real part, and small dots are the imaginary part.

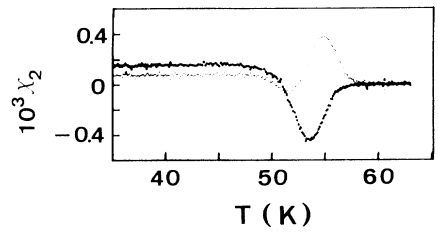

FIG. 9. Real (large dots) and imaginary (small dots) components of χ_2 as a function of temperature, where $\mu_0 H_{ac}=0.01$ mT, $H_{dc}=0$, and $f_1=132$ Hz.

demonstrated by Ishida and Goldfarb, the signs of even-n harmonic terms depend on the polarity of H_{dc} (see Figs. 15 and 16 of Ref. 11). In other words, χ_2 as a function of temperature shifts phase by π when H_{dc} changes the sign. In fact, in the present case, the use of the minus sign for H_{dc} was requested to fit the calculated χ_2-t_r curves to the observed ones. As seen in the figure, the magnitude of χ_2 tends to decrease as B_0 increases. For a further increase of B_0, χ_2 asymptotically vanishes, resulting in the Bean model. From the magnitude of χ_2, we can judge that B_0 must be much smaller than 10 mT and probably is in the vicinity of a few mT. It is also predicted from the results that B_0 should be much larger than 0.1 mT, and is consistent with the prediction made from the odd-n harmonic susceptibilities.

From the above discussion, generation of the higher-harmonic susceptibilities seems to arise from supercurrents according to the Kim-Anderson model with a finite value of B_0, but not by the weak-link model. However, there are two distinct problems to be examined. One is the magnitude of B_0, and the other is the experimental fact that the higher-harmonic terms always appear below T_{c2}, the onset temperature of the coupling phase.

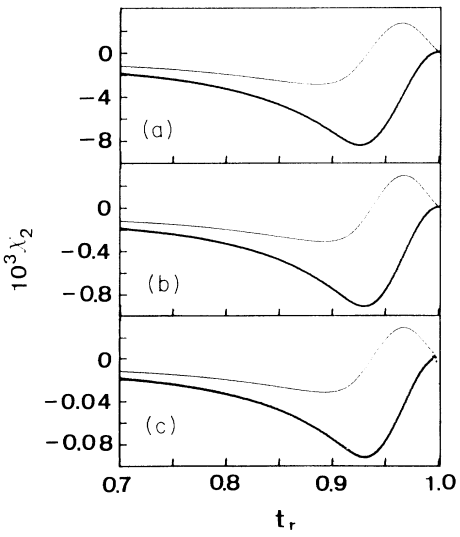

FIG. 10. χ_2 vs reduced temperature t_r calculated with use of the Kim-Anderson model with three different values of B_0, where $\mu_0 H_{ac}=0.01$ mT, $\mu_0 H_{dc}=-0.01$ mT, and $f_1=132$ Hz: (a) $B_0=0.1$ mT, (b) $B_0=1$ mT, and (c) $B_0=10$ mT.

In order to clarify these problems, we discuss the physical meaning of the *finite* value of B_0. As is well known, flux creep is the motion of bundles of flux lines caused by the Lorentz force $\mathbf{J}\times\mathbf{B}$, where $\mathbf{J}$ is the current density. For the case $B_0=0$ in Eq. (4) (the simplified Kim model), the local Lorentz force $\mathbf{J}_c\times\mathbf{B}_i$ causes flux lines to move over the pinning force. According to Anderson,[8] the constant B_0 is ascribed to the fact that the bundle of flux lines cannot contain less than a flux quantum ϕ_0, implying that B_0 would be assigned to an average flux density of a single vortex. Consequently, even for near-zero values of B_i. J will have a critical value. If $B_0 \gg B_i$ in Eq. (4), the local Lorentz force acting on an individual flux quantum is approximately given by $\mathbf{J}_c\times\mathbf{B}_0$. Anderson roughly evaluated B_0 as 200 mT, assuming that the size of the vortices is of dimension $\sim 10^{-14}$ m^2. This estimation is very close to the value observed by Kim, Hempstead, and Strnad[7] for conventional superconductors.

In contrast to the above case, our observation suggests that B_0 for sintered oxide superconductors is extremely small, probably in the vicinity of a few mT. The reason for such a small value of B_0 may come from the effective dimension of a flux quantum, which would be much bigger in sintered samples than in conventional superconductors. In sintered oxide superconductors, vortices preferentially appear near intergrain weak-link junctions, because flux lines are excluded from the bulk grains as long as the applied magnetic field is less than the intrinsic lower critical field. In such a case, the vortex size is approximately given by $2\lambda L$, where λ is the London penetration depth and L is the length of the junctions, which is expected to be nearly the same size as that of the grains. Assuming[21–23] $\lambda=3000$ Å and $L=3$ μm, $B_0=\phi_0/2\lambda L$ is estimated to be about 1 mT, which is on the same order as our observations.

Despite the reasonable value of B_0 derived by taking into account the size of weak-link junctions, the weak-link model failed to describe the observed χ_n-t_r profiles, as shown in Figs. 3(d), 4(d), and 5(d). The reason might be the incorrect assumption that the specimen as a whole behaves like a single loop because of its coherent nature. Assuming that the specimen involves a number of coaxial weak-link loops ($j=1,2,\ldots,m$), we consider, phenomenologically, the magnetic response of the specimen against an applied ac field. When the applied field starts to increase from zero, the flux is, at the initial stage, completely excluded by the shielding supercurrent through the outermost loop, I_{c1}. When the field amplitude exceeds the critical value which induces I_{c1}, the flux penetrates into this loop. As the field amplitude increases, the flux penetration occurs sequentially, and thus the distribution of the magnetic-flux density in the specimen becomes steplike, discretely jumping by ΔB_j, which is proportional to the critical-current density of the jth loop, I_{cj}. Suppose ΔB_j is very small and the number of coaxial loops, m, is sufficiently large; then the distribution of the flux density inside the specimen can be approxi-

mated by a continuous line. In addition, if ΔB_j is constant for all the coaxial loops, the field distribution becomes a straight line, which is equivalent to the Bean model. However, if I_{cj} is inversely proportional to $(B_0+|B_i|)$, the distribution of the flux density obeys the Kim-Anderson model. In this manner, assuming a large number of coaxial loops surrounding the specimen, instead of a single loop, the extended weak-link model may be treated as algebraically equivalent to the critical-state model.

We must emphasize, however, that there is an essential difference in the asymptotic equivalence between these two models regarding the origin of pinning force. In the critical-state model, the pinning force is believed to arise from inhomogeneity, dislocations, and other physical defects involved in the specimen, while in the extended weak-link model, the critical-current density I_{cj}, i.e., the strength of weak links at the intergrains, regulates the flux motion, and this eventually explains why the higher-harmonic terms of sintered oxide superconductors appear below T_{c2}.

We expect the extended weak-link model, in which a number of coaxial weak-link loops are taken into consideration, to be more useful for analyses of the magnetic response of oxide superconductors prepared by sintering. This conclusion seems to be closely related to the work by Jeffries *et al.*,[24] who studied bulk YBCO powder and pellets and found semiquantitative agreement with the predictions of a dynamical model of the material as a suitably averaged ensemble of prototype flux-quantized loops with weak links.

V. CONCLUSIONS

We measured the superconducting transition of a sintered $YBa_2(Cu_{0.94}Fe_{0.06})_3O_y$ pellet in terms of harmonic ac susceptibilities χ_n ($n=1$, 2, 3, 5, and 7). The fundamental ac susceptibility of this material showed essentially the same profile as that of $YBa_2Cu_3O_y$ without Fe impurities, except for the transition temperature. The higher-harmonic susceptibilities measured as a function of temperature showed complicated, but nonzero values in the temperature region below the onset temperature of the coupling phase.

Analyses of the results were made in the framework of the Kim-Anderson[7,8] and Ishida-Mazaki[9] models. Comparison of the observed χ_n behaviors with the calculated results suggests that the Kim-Anderson model with B_0 values in the vicinity of a few mT reproduces the data well. However, because the magnitude of B_0 is much smaller than those for conventional superconductors and because the higher-harmonic components appear below the onset temperature of the coupling phase, an extended weak-link model modified by assuming a number of coaxial weak-link loops in the specimen would be more appropriate for the analysis of the magnetic response of sintered oxide superconductors.

An obvious follow-up experiment is to provide shielding from the Earth's field in order to reduce the ambient dc field to $\ll 0.01$ mT so that one can determine whether χ_2 vanishes.

ACKNOWLEDGMENTS

We are grateful to Dr. R. B. Goldfarb of the National Institute of Standards and Technology for valuable discussions and suggestions. The authors also express their thanks to T. Takada and Y. Bando of Kyoto University for their encouragement throughout the present work.

[1]E. Maxwell and M. Strongin, Phys. Rev. Lett. **10**, 212 (1963).
[2]T. Ishida and H. Mazaki, Phys. Rev. B **20**, 131 (1979).
[3]A. F. Khoder, Phys. Lett. **94A**, 378 (1983).
[4]R. A. Hein, Phys. Rev. B **33**, 7539 (1986).
[5]H. Mazaki, M. Tanaka, R. Kanno, and Y. Takeda, Jpn. J. Appl. Phys. **26**, L780 (1987).
[6]C. P. Bean, Rev. Mod. Phys. **36**, 31 (1964).
[7]Y. B. Kim, C. F. Hempstead, and A. R. Strnad, Phys. Rev. Lett. **9**, 306 (1962).
[8]P. W. Anderson, Phys. Rev. Lett. **9**, 309 (1962).
[9]T. Ishida and H. Mazaki, J. Appl. Phys. **52**, 6798 (1981).
[10]R. W. Rollins and J. Silcox, Phys. Rev. **155**, 404 (1967).
[11]T. Ishida and R. B. Goldfarb, Phys. Rev. B **41**, 8937 (1990).
[12]L. Ji, R. H. Sohn, G. C. Spalding, C. J. Lobb, and M. Tinkham, Phys. Rev. B **40**, 10 936 (1989).
[13]H. Mazaki, S. Katsuyama, H. Yasuoka, Y. Ueda, and K. Kosuge, Jpn. J. Appl. Phys. **28**, L1909 (1989).
[14]S. Katsuyama, Y. Ueda, and K. Kosuge, Mater. Res. Bull. **24**, 603 (1989).
[15]D.-X. Chen and R. B. Goldfarb, J. Appl. Phys. **66**, 2489 (1989).
[16]J. H. P. Watson, J. Appl. Phys. **39**, 3406 (1968).
[17]F. Irie and K. Yamafuji, J. Phys. Soc. Jpn. **23**, 255 (1967).
[18]I. M. Green and P. Hlawiczka, Proc. IEEE **114**, 1329 (1967).
[19]K. Yamamoto, H. Mazaki, and H. Yasuoka, Phys. Rev. B (to be published).
[20]K.-H. Müller, Physica C **159**, 717 (1989).
[21]D. R. Harshman, G. Aeppli, E. J. Ansaldo, B. Batlogg, J. H. Brewer, J. F. Carolan, R. J. Cava, M. Celio, A. C. D. Chaklader, W. N. Hardy, S. R. Kreitzman, G. M. Luke, D. R. Noakes, and M. Senba, Phys. Rev. B **36**, 2386 (1987).
[22]R. J. Cava, B. Batlogg, R. B. van Dover, D. W. Murphy, S. Sunshine, T. Siegrist, J. P. Remeika, E. A. Rietman, S. Zahurak, and G. P. Espinosa, Phys. Rev. Lett. **58**, 1676 (1987).
[23]J. T. Markert, T. W. Noh, S. E. Urssek, and R. M. Cotts, Solid State Commun. **63**, 847 (1987).
[24]C. D. Jeffries, Q. H. Lam, Y. Kim, C. M. Kim, and A. Zettl, Phys. Rev. B **39**, 11 526 (1989).